Effects of Supercoiling in Electrophoretic Trapping of Circular DNA in Polyacrylamide Gels

ARTICLE *in* BIOPHYSICAL JOURNAL · JULY 1998

Impact Factor: 3.97 · DOI: 10.1016/S0006-3495(98)78020-8 · Source: PubMed

1 AUTHOR:

Björn Akerman
Chalmers University of Technology
78 PUBLICATIONS **1,726** CITATIONS

SEE PROFILE

Effects of Supercoiling in Electrophoretic Trapping of Circular DNA in Polyacrylamide Gels

Björn Åkerman
Department of Physical Chemistry, Chalmers University of Technology, S-412 96 Göteborg, Sweden

ABSTRACT Electrophoretic velocity and orientation have been used to study the electric-field-induced trapping of supercoiled and relaxed circular DNA (2926 and 5386 bp) in polyacrylamide gels (5% T, 3.3% C) at 7.5–22.5 V/cm, using as controls linear molecules of either the same contour length or the same radius of gyration. The circle-specific trapping is reversible. From the duration of the reverse pulse needed to detrap the molecules, the average trap depth is estimated to be 90 Å, which is consistent with the molecular charge and the field strengths needed to keep molecules trapped. Trapped circles exhibit a strong field alignment compared to the linear form, and there is a good correlation between the enhanced field alignment for the circles and the onset of trapping in both constant and pulsed fields. The circles do not exhibit the orientation overshoot response to a field pulse seen with linear DNA, and the rate of orientation growth scales as $E^{-2 \pm 0.1}$ with the field, as opposed to $E^{-1.1 \pm 0.1}$ for the linear form. These results show that the linear form migrates by cyclic reptation, whereas the circles most likely are trapped by impalement on gel fibers. This proposal is supported by very similar velocity and orientation behavior of circular DNA in agarose gels, where impalement has been deemed more likely because of stiffer gel fibers. The trapping efficiency is sensitive to DNA topology, as expected for impalement. In polyacrylamide the supercoiled form (superhelical density $\sigma = -0.05$) has a two- to fourfold lower probability of trapping than the corresponding relaxed species, whereas in agarose gels the supercoiled form is not trapped at all. These results are consistent with existing data on the average holes in the plectonemic supercoiled structures and the fiber thicknesses in the two gel types. On the basis of the topology effect, it is argued that impalement during pulsed-field electrophoresis in polyacrylamide gels may be useful for the separation of more intricate DNA structures such as knots. The results also indicate that linear dichroism on field-aligned molecules can be used to measure the supercoiling angle, if relaxed DNA circles are used as controls for the global degree of orientation.

INTRODUCTION

Gel electrophoresis is increasingly used to study nonlinear DNA structures such as circular (Kahn et al., 1994), branched (Lilley and Clegg, 1993; Seeman and Kallenbach, 1994), bent (Crothers and Drak, 1992; Niederweis et al., 1994), knotted (Du et al., 1995), and cube-shaped (Chen and Seeman, 1991) DNA. In all of these studies, polyacrylamide gels were used as the separation matrix. Compared to agarose gels (see Nordén et al., 1991; Zimm and Levene, 1992; Åkerman, 1996a; for reviews) few mechanistic studies have been performed on DNA migration in polyacrylamide gels (Åkerman et al., 1985; Jonsson et al., 1988; Calladine et al., 1991; Sturm et al., 1996). In view of the increasing importance of electrophoretic analysis of nonlinear DNA structures in polyacrylamide, we are currently undertaking studies of the migration dynamics of circular double-stranded DNA in this gel, using linear DNA of the same size as a reference. Both nicked and supercoiled circles are being studied, to introduce some degree of molecular complexity reminiscent of the more intricate DNA structures. It should be noted that the relaxed circles we use are nicked as opposed to covalently closed. Hagerman and co-workers (Mills et al., 1994) have shown, however, that whereas removal of one base increases the flexibility of (linear) DNA substantially, a nick has very little effect, as monitored by electrophoresis in polyacrylamide gels of a composition similar to that used in the present work.

Here we present results on circle-specific traps in the polyacrylamide gel, which exhibits a preference for a relaxed DNA topology. In the strong electrophoretic fields studied here, the trapping dominates the circle behavior in polyacrylamide gels. In weaker fields (Åkerman, manuscript submitted for publication) the migration is a complex mixture of such trapping and transport involving an unexpected orientation of the DNA chains perpendicular to the field direction.

MATERIALS AND METHODS

DNA and gel samples

All experiments were performed in TBE buffer (50 mM Tris, 50 mM borate, 1.25 mM EDTA, pH 8.2) at 20°C. Polyacrylamide (Biorad) gels were 5% T and 3.3% C. Agarose gels (Biorad, DNA grade) were 1%. Supercoiled and nicked forms of ΦX174 DNA (5386 bp) were from New England Biolabs, and those of pIBI30 DNA (2926 bp) from IBI. The pIBI30 was linearized with *Eco*RI restriction endonuclease, and linear fragments 1353 bp in length were from a *Hae*III digest of ΦX174 (Pharmacia). The supercoiled samples contained 5% nicked circles, the nicked samples 10% linear DNA. Col1 plasmid DNA (10,900 bp) was from Sigma, and contained 60% supercoil and 40% nicked circles. DNA concentrations in nucleotides are from absorption at 260 nm, using an extinction coefficient of 6600 M^{-1} cm^{-1}.

Received for publication 3 November 1997 and in final form 17 February 1998.

Address reprint requests to Dr. Björn Åkerman, Department of Physical Chemistry, Chalmers University of Technology, S-412 96 Göteborg, Sweden. Tel.: 46-31-772-3052; Fax: 46-31-772-3858; E-mail: baa@phc.chalmers.se.

0006-3495/98/06/3140/12 $2.00

The degree of supercoiling was estimated by an ethidium bromide (EB) unwinding assay in agarose gels (Poddar and Maniloff, 1984), in which the binding ratio is controlled by the EB concentration in the electrophoresis buffer. The mobility of the supercoiled form was equal to that of the nicked species at an EB binding ratio of 0.035 drug molecules per base for pIBI and 0.040 for ΦX174, the latter in good agreement with earlier results obtained with other techniques (Waring, 1970). These values correspond to 14.6 and 31.2 negative superhelical turns per molecule, respectively, if an EB unwinding angle of 26° is assumed (Keller, 1975), or to superhelical densities σ (Vologodskii and Cozzarelli, 1994) of −0.053 and −0.061, respectively, assuming 10.5 bp per turn of DNA helix.

All experiments have been performed on native DNA, without ethidium bromide staining. Table 1 shows the calculated radii of gyration (Bloomfield et al., 1974) of the linear and relaxed circular forms of the employed DNA sizes. At the present degrees of supercoiling, the radius of gyration of the supercoiled forms can be expected to be ~20% lower than for the nicked circle (Vologodskii and Cozzarelli, 1994). The nicked pIBI circles could thus be compared with linear molecules of either the same contour length (pIBI) or half the contour length, but approximately the same radius of gyration (1353 bp), and the ΦX174 circles with linear molecules of the same radius of gyration and approximately half the contour length (pIBI).

Velocity

Slab gels 2 mm thick were run in submarine mode and stained with ethidium bromide. Field strengths were as measured in the gel, and temperature was maintained at 20 ± 1°C by extensive circulation of the buffer through a heat exchanger in a water bath. In velocity experiments a sharp (<1 mm wide) starting zone ~2 mm into the gel was obtained by a 5-min prerun with field inversion gel electrophoresis (T_+ = 1 s, T_- = 0.1 s) at 22.5 V/cm. For each experiment two identical gels (containing the same amount of linear, circular, and supercoiled DNA) were run in parallel in the same electrophoresis cell, to ensure identical electrophoresis conditions for the two gels. One of the gels was removed after the introductory field inversion gel electrophoresis (FIGE) step, and stained separately with ethidium bromide. This gel was used to determine the starting position of the DNA for the velocity experiment, which was performed in the unstained second gel to have the DNA in the native state. In a few control experiments both gels were removed after the FIGE step and stained. The position of the DNA was identical in the two gels, confirming that the first gel can be used for determining the starting position.

The presented electrophoretic velocities were calculated as the distance migrated in the gel relative to this starting position, divided by the effective running time, T_{eff}. In constant field (CF) electrophoresis T_{eff} was equal to the actual running time T_{run}, whereas in FIGE, $T_{eff} = T_{run}\,(T_+ - T_-)/(T_+ + T_-)$.

Linear dichroism

Gels in a vertical cell were prepared, and linear dichroism (LD) was measured, as described in detail earlier (Jonsson et al., 1988). The (nonstained) DNA is introduced as a zone into the measuring position in the gel, by using FIGE, which separates linear and circular DNA, which ensures that measurements are performed on topologically pure samples. Each DNA type (size and topology) was studied in at least two different and freshly prepared gels.

TABLE 1 Radii of gyration (Å) of the used DNA*

R_G (Å)	ΦX174	pIBI	1353 bp
Linear	1700	1200	750
Nicked circle	1200	840	Not studied

*Calculated from wormlike chain model with persistence length 500 Å and without excluded volume effects.

LD (Nordén et al., 1991) is the difference in absorption of light plane-polarized parallel ($A_\parallel$) and perpendicular ($A_\perp$) to the direction of the electric field:

$$LD = A_\parallel - A_\perp \quad (1)$$

LD can be used to measure the average degree of DNA-helix orientation in terms of an orientation factor S, which is related to the angle θ between the helix axis and the field direction:

$$S = \langle 3\cos^2\theta - 1\rangle/2 \quad (2)$$

If the preferred helix alignment is along the electric field, S is positive, whereas a negative S indicates a net orientation perpendicular to the field (Nordén et al., 1991). S is equal to 1 if all molecules are perfectly aligned with the field (θ = 0°); if the helix axis orientation is random, S = 0; and if $S = -½$, all molecules are oriented with their helix axis perpendicular to the field direction (θ = 90°). S is obtained by dividing the LD by the isotropic absorption (A_{iso}) of the sample when the DNA molecules are randomly oriented (absence of field) (Nordén et al., 1991):

$$LD/A_{iso} = -1.48S \quad (3)$$

The negative sign of the so-called optical factor, −1.48 in Eq. 3, reflects the nearly perpendicular orientation of the transition moments with respect to the DNA helix axis in B-DNA (Nordén et al., 1992), which is the secondary structure DNA attains in polyacrylamide gels (Åkerman et al., 1985).

Rather long pulses are required to obtain a steady-state LD signal for the circles (see Results), and this caused the concern that electrophoretic transport may change the concentration of DNA at the measuring position, which would contribute to the measured LD time profile through A_{iso} in Eq. 3. Measurements of A_{iso} (at 260 nm in the absence of field) before and after field pulses, using the same beam configuration as in LD, was therefore used to confirm that there was no detectable change in DNA concentration during the pulses. The LD time traces from the Jasco 500 instrument were recorded with a Nicolet digital oscilloscope for averaging (4–10 traces per measuring condition) and for further analysis by computer. All kinetic data have been checked for potential artefacts from limitations in the sampling frequency or the JASCO instrument time constant.

RESULTS AND DISCUSSION

Velocity measurements

The electrophoretic velocity shows distinct differences between circular and linear DNA molecules in polyacrylamide gels. Fig. 1 shows the result of a velocity experiment with ΦX174 DNA at 22.5 V/cm at three different DNA concentrations. The gel in Fig. 1 *a* was removed from the electrophoresis cell after the prerun with field inversion gel electrophoresis, to determine the starting position of the DNA zones. At all three concentrations, the supercoiled and nicked starting positions are ~2 mm into the gel from the wells. The linear form is seen as a minor component in the nicked sample, and its starting position is less than 0.5 mm further downfield compared to that of the circular forms. The gel in Fig. 1 *b* (which includes a fourth intermediate DNA concentration) shows the zone positions after an additional 60 min of constant field electrophoresis. For the nicked circle, the zone remains at the starting position at all DNA concentrations. A majority of the loaded supercoiled DNA is also found at the starting position, but a rapidly fading smear extends 3–4 mm downfield from the starting position. In contrast, the linear molecules form a narrow

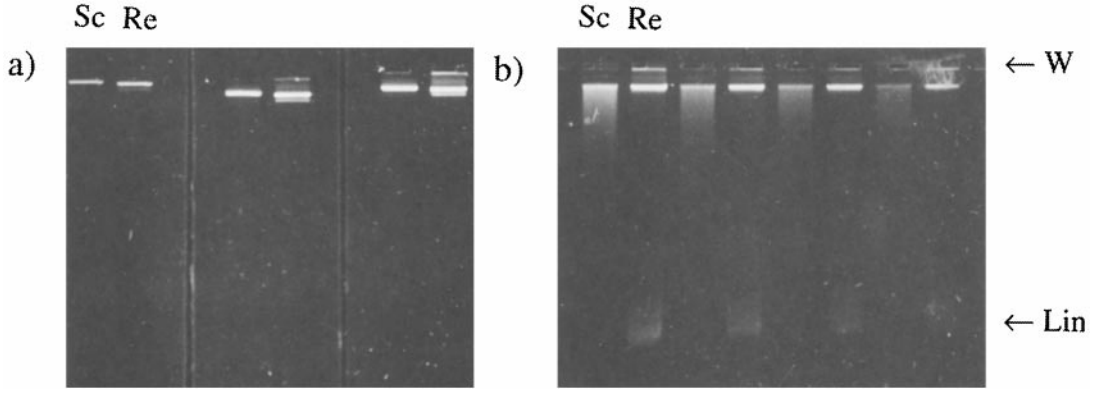

FIGURE 1 Electrophoretic trapping of nicked (Re) and supercoiled (Sc) circular ΦX174 DNA (5386 bp) in polyacrylamide gel in a constant electric field. The linear form (Lin) is present as a minor component in the nicked sample. (*a*) Position of zones after prerun with FIGE for 5 min (see Materials and Methods). DNA concentrations in pairs of lanes from left to right: 40 μM, 160 μM, and 320 μM. (*b*) Position of zones after constant field electrophoresis (22.5 V/cm) for 1 h. DNA concentrations in pairs of lanes from left to right: 320 μM, 160 μM, 60 μM, and 40 μM. W is the position of the wells.

zone well beyond the starting position at all concentrations. (The velocity of the linear form increases slightly with increasing DNA concentration, but the mechanism behind this effect has not been investigated here.)

The results of Fig. 1 indicate that at 22.5 V/cm the circles come to full arrest by being trapped at the starting position. This was confirmed by repeating the experiment with six identically loaded gels (including one control for starting position) and removing the gels after different durations of the constant field electrophoresis at 22.5 V/cm. When zone position is plotted versus time (*open symbols* in Fig. 2), the linear form exhibits a constant velocity, reflecting normal migration. In contrast, the zones of both circular forms remained at the positions at which they had arrived after the 5-min prerun by FIGE. No further migration was detected, even after several hours of electrophoresis.

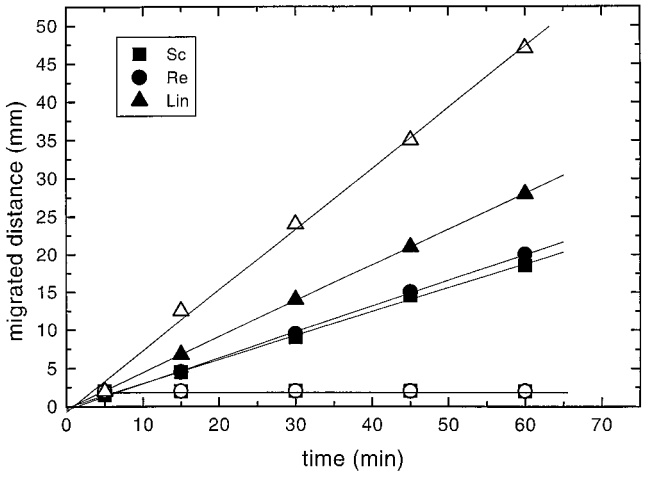

FIGURE 2 Migrated distance in polyacrylamide gel versus time for linear (Lin), relaxed (Re), and supercoiled (Sc) ΦX174 DNA in constant field (*open symbols*) and field inversion gel electrophoresis (FIGE) (T_+ = 1 s, T_- = 0.1 s; *closed symbols*). Uncertainty is less than the size of the symbols.

To our knowledge, this is the first report of circle-specific trapping in polyacrylamide gels. In one of the comparatively few systematic studies of electrophoretic migration of circular DNA in polyacrylamide gels, Harley et al. (1973) showed that SV40 DNA (4000 bp) migrates with low and strongly decreasing mobility in 2–3.5% polyacrylamide gels at 14 V/cm, but full arrest was not observed. Broad zones was found by Bishop et al. (1967) for double-stranded ΦX174 in 2.4% gels at 5.5 V/cm, but again no arrest was reported. The arrest observed here is for larger DNA, higher field, and/or denser gel, of which at least the first two factors are shown here to promote trapping.

The present study focuses on how the topological state of the circles affects the trapping behavior. Both supercoiled and nicked circles are trapped, but there are differences (Fig. 1). The somewhat extended trapping zones formed by the supercoiled species suggest that they are less efficiently trapped than the nicked form, which was immobilized at the starting position (i.e., the width of the trapped zone was the same as that of the starting zone within the experimental resolution). It is important to note that there was no significant difference in the distribution (i.e., relative fluorescence intensity) of the trapped molecules when the DNA concentration was increased by eightfold, from 40 μM to 320 μM. Therefore, at least in this DNA concentration range, the extended zone shape for the supercoiled species is not an effect of lack of trapping sites, but reflects a difference compared to the nicked circles that is inherent to the trapping of individual molecules.

In field inversion gel electrophoresis with a 1-s forward pulse time and a 0.1-s backward pulse time, both types of circles migrate as narrow zones (Fig. 3), as does the linear DNA. The velocity is constant as a function of time (Fig. 2, *solid symbols*), reflecting normal migration for times that are long compared to the trapping time of the circles in a constant field. Furthermore, when such pulsed fields are applied after the molecules have been trapped by a constant field (22.5 V/cm), both circular forms migrated normally

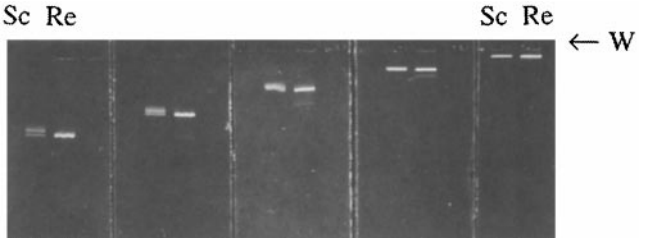

FIGURE 3 Electrophoretic migration in FIGE ($T_+ = 1$ s, $T_- = 0.1$ s) of ΦX174 DNA in polyacrylamide gel. Five gels were loaded with 10 μl of 40 μM supercoiled (Sc) and nicked (Re) DNA, and were subjected to (*from right to left*) 5, 15, 30, 45, and 60 min of electrophoresis. W is the position of the wells.

(not shown). This observation is important, because it shows that a backward pulse can detrap the molecules and thus that the field-induced arrest is reversible. In pulsed fields the velocities of both circles were lower than for the linear form, and under the present pulsing conditions the supercoiled species exhibited a slightly lower velocity than the relaxed form (Fig. 2, *solid symbols*). The difference in velocity between the topological forms was dependent on pulsing conditions, however.

Both the circles migrate if the forward pulse is short enough, and the backward pulse long enough. With a fixed forward pulse duration of $T_+ = 1$ s, the effect of the duration of the backward pulse ($T_- < T_+$) (Fig. 4 *a*) is quite distinct and very similar for the two topological forms. Below a critical backward pulse duration of $T_-^c \approx 5$ ms (including the CF case), the molecules are immobilized. When T_- is longer than T_-^c, the molecules move (as a sharp zone), and for $T_- > 50$ ms the velocity is essentially constant (at the level reported in Fig. 2).

Stronger topological effects were observed if the forward pulse time instead was varied ($T_+ > T_-$), with the backward pulse time being held constant (Fig. 4 *b*). The value $T_- = 100$ ms was chosen because it is long enough to allow migration, according to Fig. 4 *a*. For short forward pulses there is an approximate velocity plateau that is similar for the two forms, and equal to that observed for long enough backward pulses in Fig. 4 *a*. From this level the velocity decreases only gradually (compared to the effect of the reverse pulse) to zero as the forward pulses are made longer, and in a manner that depends on topology. It occurs between 1 and 100 s for the relaxed form, and later for the supercoiled form, approximately between 10 and 1000 s. This pattern, including the topology effect, is retained if the (still fixed) T_- is increased to 200 ms (not shown), which also allows migration according to Fig. 4 *a*.

It is important to note that the velocity only starts to decrease if the forward pulses are longer than ~0.5 s. The value $T_+ = 1$ s was therefore used in Fig. 4 *a*, so that the molecules start to become hooked during the forward pulse. In this way the possibility of migration in the experiments with constant T_+ will depend on the backward pulse being long enough to detrap the molecules during each cycle. For shorter reverse pulses, more and more molecules become trapped for every forward pulse, and migration ceases.

This interpretation is strongly supported by measurements of the electrophoretic orientation of the DNA, a phenomenon that turns out to be as important for explaining the behavior of circular DNA as it has been for understanding the migration of linear DNA in gels (Åkerman, 1996a).

Electrophoretic orientation in constant fields

Fig. 5 *a* shows the orientation responses $S(t)$ of nicked circular pIBI DNA ("Re") to a pulse of constant electric field of 22.5 V/cm, which is compared with the response of linear DNA of two sizes, either of the same contour length ("Lin") or of the same radius of gyration ("Lin/2") as the circular form. The orientation factor S was calculated from the LD response at 260 nm, using Eq. 3. Importantly no LD responses were observed at a wavelength of 300 nm, where DNA does not absorb light but the gel does, or at 260 nm in a DNA-free gel (not shown). This shows that there is no detectable gel orientation under these conditions, which

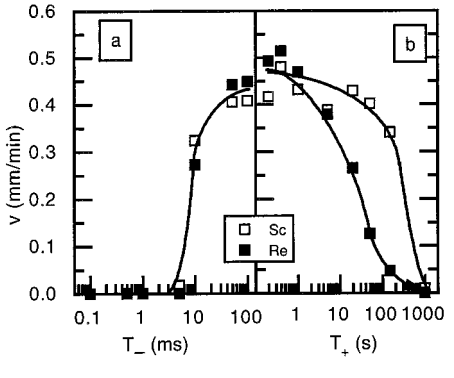

FIGURE 4 FIGE velocity in polyacrylamide gel of relaxed (Re) and supercoiled (Sc) ΦX174 DNA as a function (*a*) of backward pulse time T_- at a constant forward pulse time $T_+ = 1$ s, and (*b*) of forward pulse time T_+ at a constant backward pulse time $T_- = 100$ ms.

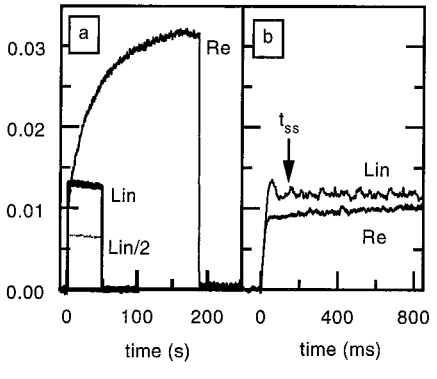

FIGURE 5 (*a*) LD response (260 nm) to field pulse (22.5 V/cm) of nicked circular (Re) and linear (L) pIBI30 DNA (2926 bp), and of linear 1353 bp DNA (Lin/2) in polyacrylamide gel. The field was applied at time 0 and turned off after 185 s (Re) or 50 s (Lin, Lin/2). (*b*) Initial part of the response at higher time resolution.

otherwise would have contributed to the 260-nm signal (Jonsson et al., 1988). The LD profile measured at 260 nm thus reflects changes in DNA orientation S with time.

Both the circular and linear forms orient with the helix axis preferentially parallel to the direction of migration ($S > 0$), confirming earlier results in the case of linear DNA (Jonsson et al., 1988). This direction of orientation is expected, because it is along the force of the electric field, but is not self-evident. Indeed, at low fields the circular DNA molecules orient perpendicular to the field direction (Åkerman, manuscript submitted for publication). Here we focus on the strong-field regime, where the direction of orientation is the same for the linear and circular forms, but where the circles differ in other aspects of the orientation.

The most prominent difference is that the rate of orientation growth is several orders of magnitude lower for the circles than for the corresponding linear form (Fig. 5 *a*), except for a fast component (rise time ~15 ms), which is seen by increasing the time resolution (Fig. 5 *b*). Second, circles do not exhibit the orientation overshoot that is seen after ~60 ms with the linear form (Fig. 5 *b*). Finally, the degree of orientation of the circles is higher than for the linear form, especially because the relevant comparison is rather with the linear form with half the contour length (1353 bp) of the circle ("Lin/2" in Fig. 5 *a*): for linear DNA the degree of electrophoretic orientation in polyacrylamide increases approximately linearly with molecular length (Jonnson et al., 1988), so a linear molecule of half the contour length can be expected to have the same effective length for migration as the circle. (A similar effective size for the circular form has been observed by Stellwagen (1988) during orientation in gels caused by stronger fields.) From Fig. 5 *a* it is seen that the 1353-bp fragment exhibits a considerably lower orientation (Fig. 5 *a*) than the pIBI circle.

These three differences between circular and linear DNA are even more accentuated for the larger ΦX174 species (Fig. 6), where at 22.5 V/cm the nicked ΦX174 circle is ~10 times more strongly oriented than its approximate linear half (i.e., pIBI, or "Lin" in Fig. 5 *a*). In addition, Fig. 6 shows two other important observations regarding the electrophoretic orientation of circular DNA in polyacrylamide gels, which will be further analyzed below. The rate of orientation growth increases strongly with increasing field. Second, DNA topology is seen to affect both the rate and degree of orientation, because the supercoiled species orients more slowly than the relaxed form, and (at 22.5 V/cm) attains a lower degree of steady-state orientation.

The presence of an overshoot (Fig. 5 *b*) means that the linear form most probably undergoes a cyclic migration similar to the one that occurs for linear DNA in agarose gels, in which the oscillatory orientation response is caused by transient and repetitive hooking of the DNA chain around gel fibers (Larsson and Åkerman, 1995). Circles are probably not oriented by such transient hooking, because they do not exhibit an overshoot (Fig. 5 *b*). Still, some kind of interaction with the gel matrix is required, because, in fact, at these low electrophoretic fields the magnitude of the orientation S is too high for a dipole mechanism (Ding et al., 1972) already for the linear form.

For ΦX174 the build-up of circle orientation (Fig. 6) occurs in the same time range of tens to hundreds of seconds, in which the forward pulse times lead to reduced velocity in FIGE (Fig. 4 *b*). Furthermore, the effect of topology is parallel between velocity and orientation build-up, because in both cases the time range is longer for the supercoiled form. From this correlation between increased orientation and reduced velocity, it is concluded that the orientation mechanism for the circles involves their immobilization, and we propose anchoring through impalement on protruding gel fibers (Fig. 7). This model for the trapping explains why the orientation is along the force of the pulling field (i.e., $S > 0$ in Figs. 5 and 6) and predicts that the orientation will be more efficient than for the corresponding linear form (Figs. 5 and 6), because the circle anchoring is not just transient. Indeed, permanent anchoring by impalement would explain how the degree of orientation of the ΦX174 circles (Fig. 6) can approach those levels observed for tethered (linear) DNA molecules, which also exhibit considerably higher orientation than their migrating counterparts (Åkerman, 1996b). Finally, impalement would explain the FIGE velocity results (Fig. 4), because backward pulses that are long enough will lift the molecules off the

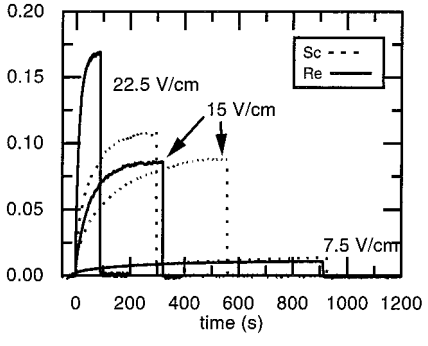

FIGURE 6 LD response (260 nm) to field pulse (of indicated strength) of nicked (Re) and supercoiled (Sc) circular ΦX174 DNA (5386 bp) in polyacrylamide gel. The field was applied at time 0.

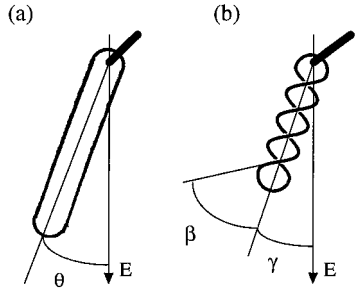

FIGURE 7 Proposed impalement traps for circular DNA. Idealized structure of impaled nicked (*a*) and supercoiled plectonemic (*b*) molecules. E is the direction of the electric field.

hook and lead to nonzero velocity (Fig. 4 *a*). This will occur unless the forward pulses are so long that molecules are detrapped for durations that are negligible compared to the time the molecules are impaled, in which case the net migration will be zero, despite the fact that the backward pulses are long enough for detrapping (Fig. 4 *b*).

The marked difference between circles and linear DNA observed in both velocity and orientation is thus consistent with an impalement model. The degree of orientation at a certain instance then reflects the number of circles that have been immobilized at that time, if it can be assumed that once hooked, all molecules of a certain size orient to the same degree at a certain field strength. Within this assumption, the rate of orientation growth then will be a measure of the probability per unit time of trapping, which can be expected to depend on gel properties such as density and lengths of trapping gel fibers, but also on DNA properties such as size and velocity (i.e., field strength). Here we are particularly interested in the differences in impalement efficiency between the two circle forms, as reflected in velocity (Figs. 1 and 4 *b*) and orientation (Fig. 6). It is important to note that all LD studies were made at DNA concentrations at which there are enough trapping sites (Fig. 1), so that the LD build-up kinetics reflect the single-molecule probability of becoming trapped.

The observation that the nicked form reaches a steady orientation much faster than the supercoiled form (Fig. 6) is important for understanding the difference in their trapping behavior (Fig. 1), and the rise kinetics was therefore studied in some detail. For both the supercoiled and nicked species, the build-up is dominated by a single exponential (Fig. 8), which represents 74% and 79% of the amplitude for the relaxed and supercoiled species, respectively, at 22.5 V/cm. The remaining 20–25% has a much faster rise time of less than 1 s (Fig. 5 *b*) and represents an orientation component related to the migration between obstacles (Åkerman, manuscript submitted for publication), as opposed to the trapping mechanism we focus on here. Furthermore, with pIBI both circle types exhibit a single exponential growth for the parallel component at long times (not shown), but the amplitude is somewhat smaller, at 65% for supercoiled and 55% for nicked. Again, the supercoiled form orients more slowly than the nicked circle, as was observed for ΦX174. The collected time constants (t_{imp}) of the dominating build-up component are given in Fig. 9 *a* (ΦX174) and Table 2 (22.5 V/cm).

The orientation growth kinetics support the assumption that circles are impaled. The fitted time constants for growth decrease rapidly with increasing field strength (Fig. 9 *a*). In fact, the power law $t_{imp} \approx E^{-2 \pm 0.1}$ (Fig. 9 *a*, *inset*) clearly indicates an orientation mechanism different from pure electrophoretic transport, which usually results in an exponent of about −1 (Åkerman, 1996a). The latter value simply reflects the field dependence of the velocity, which is the governing factor for the rate of molecular deformation (i.e., orientation) if it occurs through transport (Åkerman, 1996a). For the linear form the orientation rate can be quantified by the time t_{ss} needed to reach steady state (Åkerman et al., 1989), which decreases with increasing field strength (Fig. 9 *b*), as can be expected from the increased electrical force. In this case a value of −1.1 is observed for the slope (Fig. 9 *b*, *inset*), which is indeed close to the migration value, and therefore is in accord with the reptation mechanism proposed for the linear form. The exponent may, in fact, be more negative than −1, also for a migration mechanism due to orientation effects (Åkerman, 1996a), but even with degrees of orientation (*S*) considerably higher than those observed here, the exponent only rises to -1.2 ± 0.1 (Åkerman et al., 1989). Therefore migration alone cannot give rise to the −2 scaling law observed for circles, which supports the assumption that they are oriented by a nonmigrative mechanism, such as impalement.

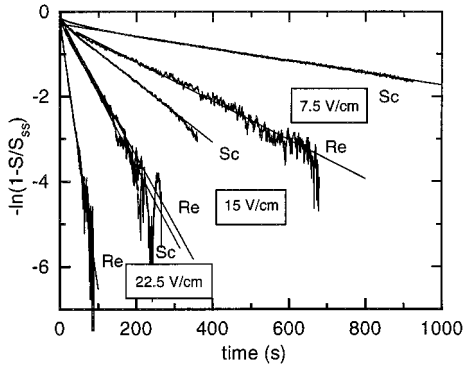

FIGURE 8 Semilogarithmic plot of orientation growth for nicked (Re) and supercoiled (Sc) ΦX174 DNA. Data are from Fig. 6. Straight lines are best fit to monoexponential growth at long times.

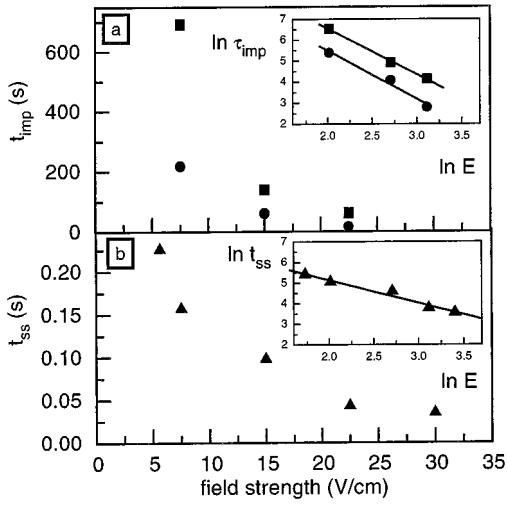

FIGURE 9 Time constants for orientation build-up versus field strength in polyacrylamide gel. (*a*) Nicked (●) and supercoiled (■) circular ΦX174 DNA. Uncertainties are smaller than the size of the symbols. t_{imp} is from the slopes of fitted monoexponential growths in Fig. 8. (*Inset*) Double-logarithmic plot, where linear regression gives the slopes -2.0 ± 0.1 in both cases. (*b*) Linear pIBI DNA. t_{ss} is the time needed to reach a steady orientation level (cf. Fig. 5 *b*). (*Inset*) Double-logarithmic plot, where the linear regression gives the slope -1.1 ± 0.1.

TABLE 2 Build-up time constant (s) for circle orientation at 22.5 V/cm*

t_{imp} (s)	ΦX174	pIBI
Supercoil	61	51.2
Nicked	17	38.6

*Obtained from slope of best linear fit in Fig. 8.

However, also for the impalement model transport effects are expected to be involved in determining the trapping rate: the higher the field, the faster the molecules will be searching for traps in which to become impaled and oriented. A contribution of approximately -1 to the E dependence of the growth rate is thus expected from transport. In addition, however, the trapping efficiency (and therefore the orientation growth rate) will depend on the concentration of suitable traps. The density of traps will increase with increasing field, because a higher field means that a shorter gel fiber suffices to overcome the potentially detrapping Brownian motion. This increase in trap density will increase the probability of trapping per unit time, and hence contribute to the E dependence of the orientation growth rate. A slope more negative than -1 is thus expected with the impalement model, but the actual value of the exponent will depend on the details of the distribution of lengths of dangling gel fibers.

Topology effects on probability of impalement

The fact that the slopes in Fig. 9 *a* (*inset*) are so similar for supercoiled and nicked circles indicates that they are oriented by the same mechanism. The difference in magnitude of the time constants for a given molecular size (Table 1) implies, however, that the impalement mechanism is less efficient for the supercoiled circles. This proposal is further supported by the observation that with the supercoiled species, the net velocity decreases more slowly with increasing forward pulse duration in FIGE (Fig. 4 *b*), and by the broader zones of trapped DNA for the supercoiled form (Fig. 1). These results show that on average, the supercoiled molecules have to migrate for longer times and/or longer distances to find a suitable trap. It is likely that the search velocities are similar for the two topological forms, because their plateau velocities in pulsed fields (Fig. 4, *a* and *b*) are similar. The difference in impalement efficiency, therefore, should not stem from the rate of finding traps, but rather the probability of trapping being lower for the supercoil once a trap has been located. The trapping force will be the same for the two forms because they have identical electrophoretic charge, so the difference in trapping probability must lie in the probability of entering the trap, rather than in the capability of remaining in it. This is appealing in the impalement model, because intuitively supercoiling should reduce the size of the holes in the DNA coil that are available for penetration by the gel fiber, and literature data on supercoiling support this interpretation.

Supercoiled DNA molecules are overwound (plectonemic) rather than toroidal (Vologodskii and Cozzarelli, 1994). Cryoelectron microscopy has been used (Bednar et al., 1994) to show that in a 2600-bp DNA with superhelical density ($\sigma = -0.05$), the average helix-helix distance (center to center) is 10 nm and 2 nm, respectively, at two ionic strengths (10 and 100 mM) that encompass the present one. Because the idealized hole diameter in the corresponding nicked circle is 280 nm, supercoiling indeed decreases the total hole area available for impalement considerably. It should still be possible however for a gel fiber to penetrate some of the individual holes, because the fiber diameters in polyacrylamide gels are only 2–4 Å (Hecht et al., 1985). A lower but still finite impalement probability is thus expected for the supercoiled form of both the pIBI and ΦX174 DNA, which have similar supercoiling densities.

Theoretically the impalement problem has not been treated for a wormlike chain such as DNA. For a Gaussian chain the effective cross section for impaling the coil of a relaxed circular molecule on an infinitely thin rod is determined by the radius of gyration (Koniaris and Muthukumar, 1995). From this point of view it can be argued that the supercoiled molecule will present a smaller cross-sectional area for impalement than does the nicked circle, because its radius of gyration is smaller (Vologodskii and Cozzarelli, 1994). Quantitative comparison is difficult, however, because the theory is for a phantom chain and thus includes knotted conformations, which are not available to the real chain.

An elegant and related approach for probing the structure of supercoiled DNA is the catenation technique of Rybenkov et al. (1997). Linear DNA is circularized in the presence of the supercoiled DNA, and the probability of catenation reflects how open the supercoiled structure is to penetration by the linear molecule. In this case the probe is itself a DNA helix, which is a more well-characterized probe than the gel fibers used in the present study. In the catenation experiments, the effective hole size is governed by the electrostatic interactions between DNA segments (within the supercoil, but also between the probe DNA and the supercoil). In view of their lower charge density, gel fibers are likely to act more as steric probes, and gel impalement may therefore be a method complementary to catenation in studies of supercoil structure.

The effect of molecular weight on the build-up kinetics is not clear cut, as judged by the data in Table 2. For the supercoiled form, the larger DNA type is immobilized faster than the smaller, whereas for the nicked form the size effect is the opposite. These apparently contradicting trends should not be surprising, because the molecular size will act through both determinants of the rate of impalement. The search velocity will most likely be lower for a larger molecule, but the density of effective traps, on the other hand, will be higher, because shorter hooks suffice for a larger molecule because it is impaled by a larger force. With a possibly rather subtle balance between these effects, an

effect of supercoiling may be to change the size dependence compared to that of the nicked circle.

LD measurements of supercoiling angle

Table 3 gives the magnitude of the steady-state orientation factor S_{ss} at 22.5 V/cm, which is seen to be lower for the supercoiled than for the relaxed form for both ΦX174 (cf. Fig. 6) and pIBI DNA. This could be due to differences in degree of molecular field alignment between the two topological forms, but here we will investigate the possibility that the difference is related to the tertiary structure of the supercoil. Supercoiling will affect the orientation of the DNA helix with respect to the long axis of the impaled and field-aligned molecules (Fig. 7): in the supercoiled species the helix axis in the super-coil turns will be less aligned with the long axis compared to the corresponding DNA segments in the nicked circle. This reduces the net orientation of the helix axis in the supercoil with respect to the field direction (S), as measured by LD.

In addition, the long axis is not perfectly field aligned in either circle form. For the nicked circle this lack of perfect axis alignment is quantified by the S value (Eq. 2) through the angle θ (Fig. 7 *a*). For the supercoiled species (Fig. 7 *b*), both the supercoiling and the lack of perfect long-axis orientation contribute to S, and these two effects factorize because of the cylindrical symmetry of the field (Schellman and Jensen, 1987). Therefore the total orientation factor in Eq. 3 is given by $S = S_{tert}S_{axis}$, where the two new orientation factors both take the form in Eq. 2. In S_{axis}, θ in Eq. 2 is replaced by the angle γ between the supercoil long axis and the field direction (Fig. 7 *b*), and the averaging in Eq. 2 is over all molecules. The orientation factor S_{tert} reflects the tertiary structure through the angle β between the local helix axis and the long axis (Fig. 7 *b*), and the average is over the whole contour. S_{tert} for the supercoiled species can be calculated from S if it is assumed that S_{axis} is the same for nicked and supercoiled circles, a hypothesis that cannot be tested here. Under this assumption, the ratio S(supercoil)/S(nicked) will be equal to the ratio S_{tert}(supercoil)/S_{tert}(nicked). Even for the nicked circle, S_{tert} is not exactly 1, because not all helix segments can be along the long axis of the aligned molecule, because a circular molecule has to have a turn somewhere. This "end" effect is also present in the supercoiled species, and is roughly corrected for by the division of S_{tert}(supercoil) by S_{tert}(nicked).

From the steady-state level at 22.5 V/cm (Table 3), one obtains a "corrected" $S_{tert} = 0.45 \pm 0.05$ for pIBI and 0.64 ± 0.05 for ΦX174, corresponding to β values of $37 \pm 2°$ for pIBI and $30 \pm 3°$ for ΦX174. This is in good agreement with literature values for the supercoiling angle α ($\alpha = 90 - \beta$; see Fig. 1 of Vologodskii and Cozzarelli, 1994), for which several other techniques give a value of 60° for supercoiled DNA independently of the superhelical density (Vologodskii and Cozzarelli, 1994).

TABLE 3 Steady-state orientation at 22.5 V/cm*

S_{ss}	ΦX174	pIBI
Supercoil	0.108 ± 0.003	0.014 ± 0.003
Nicked	0.170 ± 0.003	0.031 ± 0.003

*From Figs. 5 and 6.

The plectonemic structure given in Fig. 7 *b* is clearly an oversimplification, because electron microscopy images often show branched supercoiled structures (Bednar et al., 1994), and the extent to which these branches are pulled out by the electric forces applied here to pierce the molecules is not known. In fact, for the ΦX174 plasmid, a field strength of 22.5 V/cm corresponds to a total electric force of 0.2 pN on the molecule (assuming an effective DNA charge of 0.05 electron charges per phosphate; see below). Single-molecule experiments (Strick et al., 1996) indicate that this is close to the force (~0.3 pN) needed to start to rearrange plectonemic structures in a supercoiled DNA with a supercoiling density of −0.05, close to the value of the present DNA samples. Thus it must be kept in mind that the distribution of the supercoiling may be perturbed by the stretching force applied in the present experiments.

Electrophoretic orientation in pulsed fields

The pulsed-field type of velocity experiments presented in Fig. 4 was also performed with LD for the supercoiled ΦX174 species. Fig. 10 a shows how the LD time response for $T_+ = 1$ s varies with the duration of the backward pulse. (The corresponding velocity data are in Fig. 4 *a*.) For a T_- of less than 1 ms, the response is indistinguishable from the constant field (CF) response. For longer backward pulses, the LD response acquires a ripple, but the envelope formed by the peak values retains the slowly growing profile that is characteristic of the CF response. The rate of growth is increasingly slower, however, as the backward pulse duration increases, and the envelope amplitude decreases to the extent that above $T_- = 20$ ms the slow growth is lost and the envelope is constant in time, but is still with a ripple.

If the amplitude of the envelope (at $t = 20$ s, normalized to the CF response) is plotted versus the logarithm of T_- (Fig. 10 *b*), there is a clear correlation with the onset, growth, and saturation of the (normalized) electrophoretic velocity (from Fig. 4 *a*). This is in accordance with the proposed impalement mechanism. Below $T_- = 1$ ms the molecules remain tightly impaled on the gel fibers, as evidenced by orientation not being affected by the back-pulses. Longer back-pulses lead to 1) some transient orientation relaxation, which explains the ripple, and to 2) unhooking (Fig. 4 *a*), which explains why the process of trapping during the net forward motion is less efficient, as reflected in the slower growth of the orientation envelope (Fig. 10 *a*). Above $T_- \approx 50$ ms, the molecules migrate essentially without trapping, because (for $T_+ = 1$ s) the circles reach the plateau velocity at this value of T_- (Fig. 4 *a*). The constant level of orientation that remains above $T_- = 20$ ms

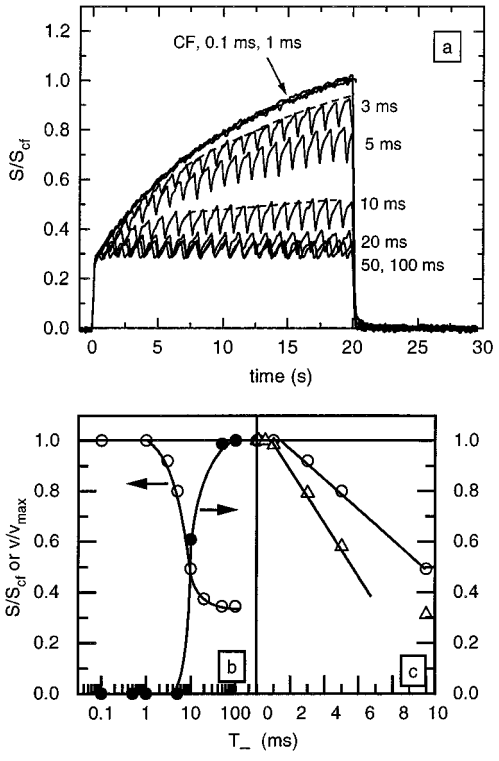

FIGURE 10 (*a*) Orientation response of supercoiled ΦX174 DNA in constant field (CF) or field inversion gel electrophoresis with different backward pulse times T_- (indicated), at a forward pulse time of $T_+ = 1$ s. LD responses were normalized at $t = 20$ s with respect to the CF-response. Polyacrylamide gel, 22.5 V/cm. (*b*) Plot of normalized LD amplitude at 20 s (*open symbols*) and normalized net electrophoretic velocity (*closed symbols*) versus logarithm of T_-. The LD data are from the envelope connecting the peak values (*dashed*) in *a*. The velocity data are from Fig. 4 *a*, and are normalized with respect to the value at $T_- = 100$ ms. (*c*) Plot of normalized LD amplitude versus T_-, for $T_+ = 1$ s (○) and $T_+ = 0.2$ s (△).

is therefore ascribed to a migrative mechanism (Åkerman, manuscript submitted for publication).

A linear plot of the normalized LD amplitude versus pulse time (Fig. 10 *c*) gives a more precise value of the critical backward time of $T_- = 1.3 \pm 0.2$ ms (for two different T_+ values), below which the response is indistinguishable from the CF response. This critical time represents the (backward) migration time that is necessary for unhooking, because the CF response is expected if no molecules are detrapped during the reverse phase, and more and more molecules are becoming trapped with each pulse cycle.

Furthermore, the experiments with constant T_- (velocity data are in Fig. 4 *b*) was performed with LD. For T_- fixed at 0.3 s (Fig. 11 *a*), $T_+ = 0.3$ s gives rise to a constant response at the same level as observed for long enough T_- in Fig. 10 *a*. For longer forward pulses ($T_+ = 1$ s, 2 s, and 5 s), a sawtooth pattern is observed that reflects the slow growth during each field pulse, with larger amplitude as T_+ increases and more molecules become impaled during each pulse. At each field reversal the orientation drops to a minimum that corresponds to the constant level observed with $T_+ = 0.3$ s.

This experiment was repeated with different values of T_-, and the maximum and minimum amplitudes are plotted versus T_+ in Fig. 11 *b*. The value of T_+ at which the saw teeth disappear, i.e., when the curves for the maximum and minimum converge, can be taken as the critical forward pulse time for hooking, because only for forward pulses longer than this value is the slow growth observed. In general, the point of convergence between the two curves depends on the chosen value of T_- (the shorter the T_-, the earlier the convergence point, as illustrated by the curves for $T_- = 5$ ms). However, the curves are very similar for different T_- values above 50 ms, which indicates the existence of a well-defined critical T_+. The data for T_- equal to 0.2 and 0.3 s agree on a critical forward pulse time of 180 ± 40 ms, which is comparable to the value of ~0.5 s obtained from velocity experiments (Fig. 4 *b*).

Characterization of the traps

In the impalement model the energy depth (U_{trap}) of a trap is given by the length of the protruding gel fiber (l_f) according to

$$U_{trap} = qNEl_f \quad (4)$$

where q is the effective charge per base pair, N is the number of base pairs, and E is the electric field strength.

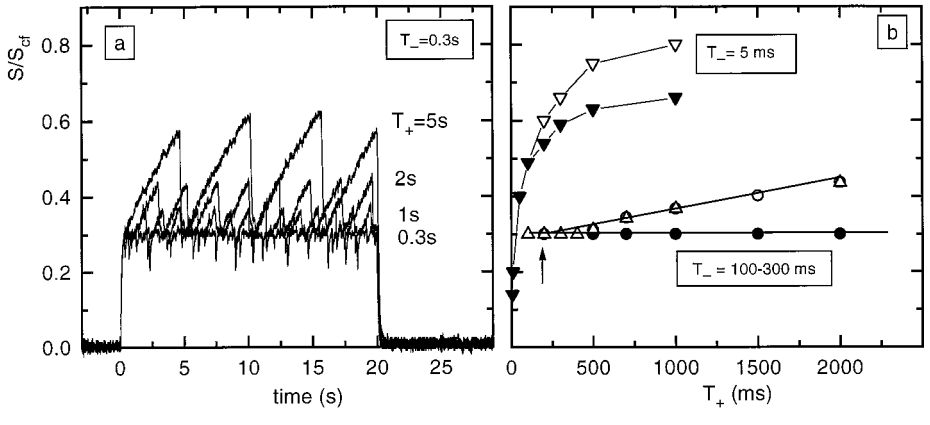

FIGURE 11 (*a*) Orientation response of supercoiled ΦX174 DNA in field inversion gel electrophoresis with different forward pulse times T_+ (indicated), at a backward pulse time of $T_- = 0.3$ s. (*b*) Plot of maximum (*open symbols*) and minimum (*closed symbols*) LD amplitudes versus T_+, at different T: ▼, ▽, 5 ms; △, 100 ms; ○, ●, 200 ms; □, 300 ms. Polyacrylamide gel, 22.5 V/cm.

The effective fiber length in the trap (l_f) can be estimated from the critical unhooking time, if the velocity of the circles during the backward pulse is known. The plateau velocity in Fig. 4 corresponds to an electrophoretic mobility of 3.0×10^{-5} cm^2V^{-1} s^{-1} at 22.5 V/cm. This is a factor of 10 lower than the free solution value for double-stranded DNA (Åkerman, 1996a), which indicates a substantial additional friction from the matrix (even without trapping), as might be expected from the size of these molecules being comparatively large for electrophoresis in polyacrylamide gels. The plateau value was therefore used as the velocity of the DNA on its way off the hook. The resulting fiber length l_f is 8.7 or 33 nm, depending on whether the critical backward pulse time is taken from the LD (1.3 ms; Fig. 10 *b*) or the velocity (5 ms; Fig. 4 *a*) experiments. These distances are surprisingly long if they are to represent the length of a gel fiber that is stiff enough to be capable of piercing and holding a DNA circle, and it is noteworthy that they would be even longer if the effective mobility in the gel were closer to the free solution value.

Such fiber lengths are necessary, however, for impalement to be able to trap DNA molecules of the sizes used here. This can be seen by comparing U_{trap} in Eq. 4 with kT, the thermal energy available for Brownian escape. The impaling force depends on the effective value for the charge per DNA phosphate, which is under debate. Smith and Bendich (1990) obtained a value of 0.1 electron charges per base pair from stretching circular molecules that were impaled on the surface of an agarose gel, a situation similar to the one proposed here to occur inside the polyacrylamide gel. Conventional electrophoretic measurements in solution indicate a value of 0.5 (Schellman and Stigter, 1977), and Stigter (1991) has argued that the low value obtained with tethered DNA is partly due to hydrodynamic flows that counteract the stretching electric force. In our case the DNA is effectively tethered too, but the hydrodynamic flows may well be shielded if the DNA molecules are inside the gel (Stigter, 1991), although Gosnell and Zimm (1993) have obtained a similarly low value of ~0.05 for molecules that migrate inside an agarose gel.

At $E = 22.5$ V/cm, a charge value of $q = 0.05$ per phosphate gives $U/kT = 0.4$ and 1.5, with $l_f = 8.7$ and 33 nm, respectively, whereas if $q = 0.5$, a fiber length $l_f = 8.7$ nm gives $U/kT = 4.0$. The estimated fiber lengths in the traps are thus consistent with field-induced arrest of the molecules, but the fibers could not be much shorter than 10 nm if the lower effective charge is a reality. It is therefore interesting that at fields not much lower than 22.5 V/cm, the zones do move, albeit with a considerable broadening (Åkerman, manuscript submitted for publication), as expected if the trapping force is insufficient, to impale the molecules permanently.

It is also possible to calculate a characteristic distance from the minimum forward pulse time that causes trapping, which on the basis of the value 180 ms obtained from the LD results (Fig. 11 *b*), becomes 1.1 μm. This value should represent some average distance to the first trap and suggests that the molecules have to traverse several cavities before becoming impaled, because the cavity sizes are on the order of 0.1 μm (Hsu and Cohen, 1984; Hecht et al., 1985).

Trapping by impalement in agarose gels

Trapping of nicked circular DNA is well established in agarose gels, and impalement was proposed as the trapping mechanism (Mickel et al., 1977), and this model was supported by the release of the circles by reversing (Levene and Zimm, 1987) or turning off (Serwer and Hayes, 1987) the field. A few of the LD and velocity experiments that proved valuable in evaluating the trapping mechanism in polyacrylamide gels were therefore repeated in agarose, using nicked Col1-plasmid DNA (10.9 kb).

In 1% agarose, the velocity in FIGE (15 V/cm) exhibited dependencies on the duration of backward and forward pulses similar to those in polyacrylamide (Fig. 4). For a constant forward pulse $T_+ = 1$ s (Fig. 12 *a*), the circles are detrapped by backward pulses longer than ~2 ms. For a constant backward pulse $T_- = 0.1$ s (Fig. 12 *b*), the velocity decreases with increasing forward pulse duration in the range of tens of seconds, in a manner similar to that of polyacrylamide.

Fig. 13 shows the LD response in agarose for three different DNA concentrations. At the two lower DNA concentrations (25 and 116 μM base), the LD response exhibits similar kinetics and degree of steady-state orientation. The dominating source of uncertainty in S is the isotropic absorbance (A_{iso} in Eq. 3), and the difference in steady-state level between the two lower concentrations is comparable to the variation observed for linear DNA between different gels (Åkerman et al., 1989). In contrast, at the highest concentration (230 μM base), the growth is significantly slower in its approach of the steady-state level, which is the same, however. These observations indicate that below a certain DNA concentration, the rate of orientation growth reflects the trapping probability of the individual molecules,

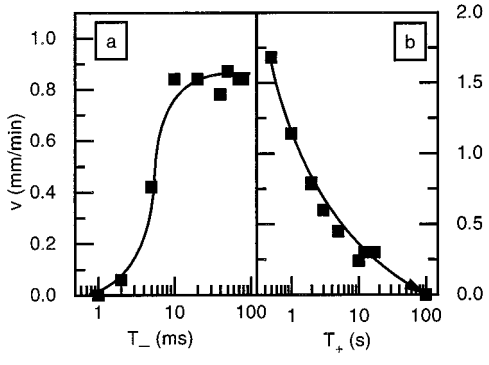

FIGURE 12 Electrophoretic velocity in 1% agarose gel of nicked circular ColE1 DNA in FIGE, as a function (*a*) of backward pulse time T_- at a constant forward pulse time $T_+ = 1$ s, and (*b*) of forward pulse time T_+ at a constant backward pulse time $T_- = 100$ ms.

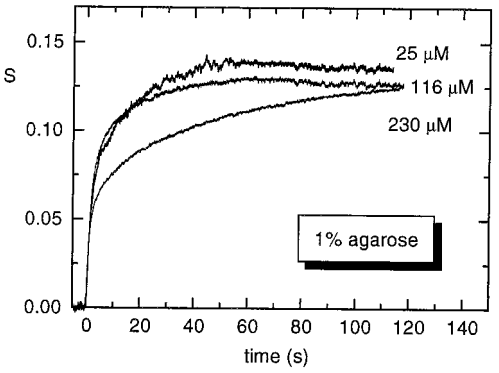

FIGURE 13 LD response (260 nm) to constant field pulse (15 V/cm) of nicked circular ColE1 DNA in 1% agarose gel at indicated DNA concentrations. The field was applied at time 0.

but that at the highest DNA concentration, there is a lack of trapping sites, so that on average, the molecules have to migrate further to find a suitable trap.

We note first that there is no orientation overshoot, in contrast to observation of the linear form under the same conditions (Magnusdottir et al., 1994), again indicating different orientation mechanisms. As in polyacrylamide, the LD shows that (at the low DNA concentrations) the DNA orientation (Fig. 13) builds up on the same time scale as the velocity falls off as a function of T_+ (Fig. 12 *b*), which establishes the trapping as the source of orientation. The final degree of orientation is the same at all concentrations, which is expected if all molecules finally become impaled. It is noticed that the degree of orientation for the circle ($S = 0.09$) is higher than for the linear form ($S = 0.04$; Magnusdottir et al., 1994) and for a linear molecule of approximately half the contour length ($S = 0.01$; Jonsson et al., 1988), under the same conditions.

The similarity in the results from polyacrylamide and agarose gels is so striking, that if impalement is the trapping mechanism in one matrix, it is also likely to be the case in the other. It can be argued that impalement seems more likely in agarose with its thicker and more rigid fibers, but the present results strongly indicate that impalement also occurs in polyacrylamide. An interesting difference between the two systems is the lack of trapping of the supercoiled species in agarose, even at 22.5 V/cm (not shown). According to the data of Bednar et al. (1994), the holes in the supercoiled structure may well be too narrow to be penetrated by the agarose gel fibers, which have a diameter of 30–90 Å (Djabourov et al., 1989; Dormoy and Candau, 1991), compared to a few Å in polyacrylamide (Hecht et al., 1985).

Relevance for the separation of nonlinear DNA structures

The results in Fig. 4 *b* demonstrate that pulsed fields of high strengths can be used to modulate the separation of different topological forms of DNA, a possibility for separation enhancement that remains to be evaluated with more intricate DNA structures, such as knots. The molecules used here are large compared to what is usually separated in polyacrylamide gels. In fact, knotted molecules of similar sizes (in terms of bp) are usually analyzed in agarose (Dean et al., 1985; Stasiak et al., 1996), but the necessary separation times are extensive. The present results show that molecules of these sizes are capable of migration as sharp zones in polyacrylamide gels if the field is pulsed. Furthermore, with a separation principle based on electrophoretic trapping, it should be possible to enhance separation rates by increasing the field strength, because the underlying impalement effect will only be enhanced by the stronger force. This is in contrast to the case in which separation is based on migration, because in conventional electrophoresis an increased field tends to make the separation poorer (cf. Nordén et al., 1991). Finally, it is learned that agarose gel fibers are rather blunt as impalement tools, compared to the fibers in the polyacrylamide gel, which therefore may be a more optimal choice of matrix for attempts to separate knots by impalement in pulsed fields.

The Swedish National Research Council is thanked for financial support and Fredrik Kjellman is thanked for performing the studies in agarose gels.

REFERENCES

Åkerman, B. 1996a. Cyclic migration of DNA in gels: DNA stretching and electrophoretic mobility. *Electrophoresis.* 17:1027–1036.

Åkerman, B. 1996b. Tethering of double-stranded DNA to agarose gels for studies of conformation dynamics during electrophoresis. *J. Chem. Soc. Chem. Comm.* 661–662.

Åkerman, B., M. Jonsson, and B. Norden. 1985. Electrophoretic orientation of DNA detected by linear dichroism spectroscopy. *J. Chem. Soc. Chem. Commun.* 422–423.

Åkerman, B., M. Jonsson, B. Norden, and M. Lalande. 1989. Orientational dynamics of T2 DNA during agarose gel electrophoresis: influence of gel concentration and electric field strength. *Biopolymers.* 28: 1541–1571.

Bednar, J., P. Furrer, A. Stasiak, J. Dubochet, E. H. Egelman, and A. D. Bates. 1994. The twist, writhe and overall shape of supercoiled DNA change during counterion-induced transition from a loosely to a tightly interwound superhelix. *J. Mol. Biol.* 235:825–847.

Bishop, D. H. L., J. R. Claybrook, and S. Spiegelman. 1967. Electrophoretic separation of viral nucleic acids on polyacrylamide gels. *J. Mol. Biol.* 26:373–387.

Bloomfield, V. A., D. M. Crothers, and I. Tinoco. 1974. Molecular weight and long range structure. *In* Physical Chemistry of Nucleic Acids. Harper and Row, New York. 159–171.

Calladine, C. R., C. M. Collis, H. R. Drew, and M. R. Mott. 1991. A study of electrophoretic mobility of DNA in agarose and polyacrylamide gels. *J. Mol. Biol.* 221:981–1005.

Chen, J., and N. C. Seeman. 1991. The electrophoretic properties of a DNA cube and its substructure catenanes. *Electrophoresis.* 12:607–611.

Crothers, D. M., and J. Drak. 1992. Global features of DNA structure by comparative gel electrophoresis. *Methods Enzymol.* 212:46–71.

Dean, F. B., A. Stasiak, T. Koller, and N. R. Cozzarelli. 1985. Duplex DNA knots produced by *Escherichia coli* topoisomerase I. *J. Biol. Chem.* 260:4975–4983.

Ding, D.-W., R. Rill, and K. E. van Holde. 1972. The dichroism of DNA in electric fields. *Biopolymers.* 11:2109–2124.

Djabourov, M., A. H. Clark, D. W. Rowlands, and S. B. Ross-Murphy. 1989. Small-angle x-ray scattering characterization of agarose sols and gels. *Macromolecules.* 22:180–188.

Dormoy, Y., and S. Candau. 1991. Transient electric birefringence study of highly dilute agarose solutions. *Biopolymers.* 31:109–117.

Du, S. M., H. Wang, Y.-C. Tse-Dingh, and N. C. Seeman. 1995. Topological transformations of synthetic DNA knots. *Biochemistry.* 34: 673–682.

Gosnell, D. L., and B. H. Zimm. 1993. Measurements of diffusion coefficients of DNA in agarose gel. *Macromolecules.* 26:1304–1308.

Harley, E. H., J. S. White, and K. R. Rees. 1973. The identification of different structural classes of nucleic acids by electrophoresis in polyacrylamide gels of different concentrations. *Biochim. Biophys. Acta.* 299:253–263.

Hecht, A.-M., R. Duplessix, and E. Geissler. 1985. Structural inhomogeneities in the range 2.5–2500 Å in polyacrylamide gels. *Macromolecules.* 18:2167–2173.

Hsu, T.-P., and C. Cohen. 1984. Observation on the structure of a polyacrylamide gel from electron micrographs. *Polymer.* 25:1419–1423.

Jonsson, M., B. Åkerman, and B. Norden. 1988. Orientation of DNA during gel electrophoresis studied with linear dichroism spectroscopy. *Biopolymers.* 27:381–414.

Kahn, J. D., E. Yun, and D. M. Chrothers. 1994. Detection of localized DNA flexibility. *Nature.* 368:163–166.

Keller, W. 1975. Determination of the number of superhelical turns in simian virus 40 DNA by gel electrophoresis. *Proc. Natl. Acad. Sci. USA.* 72:4876–4880.

Koniaris, K., and M. Muthukumar. 1995. Entanglement between a polymeric ring and a rod. *J. Chem. Phys.* 103:7136–7143.

Larsson, A., and B. Åkerman. 1995. Period times and helix alignment during the cyclic migration of DNA in electrophoresis gels studied with fluorescence microscopy. *Macromolecules.* 28:4441–4454.

Levene, S. D., and B. H. Zimm. 1987. Separations of open-circular DNA using pulsed-field electrophoresis. *Proc. Natl. Acad. Sci. USA.* 84: 4054–4057.

Lilley, D. M., and R. Clegg. 1993. The structure of branched DNA species. *Q. Rev. Biophys.* 26:131–175.

Magnusdottir, S., B. Åkerman, and M. Jonsson. 1994. DNA electrophoresis in agarose gels: three regimes of DNA migration identified and characterized by the electrophoretic orientational behaviour of the DNA. *J. Phys. Chem.* 98:2624–2633.

Mickel, S., V. Arena, and W. Bauer. 1977. Physical properties and gel electrophoresis behavior of R12-derived plasmid. *Nucleic Acids Res.* 4:1465–1482.

Mills, J. B., J. P. Cooper, and P. J. Hagerman. 1994. Electrophoretic evidence that single-stranded regions of one or more nucleotides dramatically increase the flexibility of DNA. *Biochemistry.* 33:1797–1803.

Niederweis, M., T. Lederer, and W. Hillen. 1994. Matrix effects suggest an important influence of DNA-polyacrylamide interactions on the electrophoretic mobility of DNA. *J. Biol. Chem.* 269:10156–10162.

Nordén, B., C. Elvingson, M. Jonsson, and B. Åkerman. 1991. Microscopic behaviour of DNA during electrophoresis: electrophoretic orientation. *Q. Rev. Biophys.* 24:103–164.

Norden, B., M. Kubista, and T. Kurucsev. 1992. Linear dichroism spectroscopy of nucleic acids. *Q. Rev. Biophys.* 25:51–170.

Poddar, S. K., and J. Maniloff. 1984. Measurements of DNA superhelix density by dye titration-slab gel electrophoresis. *Electrophoresis.* 5:172–173.

Rybenkov, V. V., A. V. Vologodskii, and N. R. Cozzarelli. 1997. The effect of ionic conditions on the conformations of supercoiled DNA. II. Equilibrium catenation. *J. Mol. Biol.* 267:312–323.

Schellman, J. A., and H. P. Jensen. 1987. Optical spectroscopy of oriented molecules. *Chem. Rev.* 87:1359–1399.

Schellman, J. A., and D. Stigter. 1977. Electric double-layer, zeta potential and electrophoretic charge of double-stranded DNA. *Biopolymers.* 16: 1415–1434.

Seeman, N. C., and N. R. Kallenbach. 1994. DNA branched junctions. *Annu. Rev. Biophys. Biomol. Struct.* 23:53–86.

Serwer, P., and S. J. Hayes. 1987. A voltage gradient-induced arrest of circular DNA during agarose gel electrophoresis. *Electrophoresis.* 8:244–246.

Smith, S. B., and A. J. Bendich. 1990. Electrophoretic charge density and persistence length of DNA as measured by fluorescence microscopy. *Biopolymers.* 29:1167–1173.

Stasiak, A., V. Katritch, J. Bednar, D. Michoud, and J. Dubochet. 1996. Electrophoretic mobility of DNA knots. *Nature.* 384:122.

Stellwagen, N. C. 1988. Effect of pulsed and reversing electric fields on the orientation of linear and supercoiled DNA molecules in agarose gels. *Biochemistry.* 27:6417–6424.

Stigter, D. 1991. Shielding effects of small ions in gel electrophoresis. *Biopolymers.* 31:169–176.

Strick, T. R., J.-F. Allemand, D. Bensimon, A. Bensimon, and V. Croquette. 1996. The elasticity of a single supercoiled DNA molecule. *Science.* 271:1835–1837.

Sturm, J., A. Pluen, and G. Weill. 1996. Dynamics of single-stranded DNA in polyacrylamide gels during pulsed field gel electrophoresis. A birefringence study. *Biophys. Chem.* 58:151–155.

Vologodskii, A. V., and N. R. Cozzarelli. 1994. Conformational and thermodynamic properties of supercoiled DNA. *Annu. Rev. Biophys. Biomol. Struct.* 23:609–643.

Waring, M. 1970. Variations of the supercoils in closed circular DNA by binding of antibiotics and drugs: evidence for molecular models involving intercalation. *J. Mol. Biol.* 54:247–279.

Zimm, B. H., and S. D. Levene. 1992. Problems and prospects in the theory of gel electrophoresis of DNA. *Q. Rev. Biophys.* 25:171–204.